PREDICTING THE SPECIATION AND PROPETIES OF RARE EARTH ELEMENT DURING CHEMICAL EXTRACTION FROM MINERAL DEPOSITS

By

Rasika Nimkar, Anthony Gerbino

OLI Systems, Inc. USA

Presenter and Corresponding Author

Anthony Gerbino

aj.gerbino@olisystems.com

ABSTRACT

This paper outlines the use of a modern electrolyte theory (chemistry model) to predict the chemical extraction of rare earth elements (REE) from mineral deposits. The aim is to aid the engineer in maximizing product yield and to predict secondary products formation resulting from the chemical extraction operation.

The paper includes a brief overview of the model and its departure from strong electrolyte models. It also discusses how experimental data for each the sixteen REE's differ and it effect on the ability to model these elements over different compositions and ranges. We next present the prediction of REE phase stability and speciation using extractive acids. We show the impact of impurities like high chloride concentration on extraction efficiency.

The last section of the paper contains process simulation results for REE extraction from several ore sources. The simulations include the acid digestion and chemical separation sections, and present effects of different acids and complexing agents on separating these elements from impurities.

Despite the limited validation data for REE, solution/phase predictions of the ore from which the REE's are extracted (e.g., oxides, phosphates, chlorides, silicates, etc.) are well validated. This enables accurate simulation of REE extraction from the rock matrix including the corresponding composition of the leachate and the leached ore (if critical for enhanced extraction).

Keywords: Rare Earth Elements, Extraction,

Introduction

Rare earth elements (REE) extracted from their respective source are challenged by the difficulty in separation and the ultimate value of their product. The commercial value of oxides like Nd_2O_3 and Pr_2O_3 (on the order of $USD40,000 to 50,000/ton[1]) enable more flexibility in extraction: Nd from phosphate rock tailings; Pr from bastnaesite, or Nd and Pr from Samarskite. Since extraction requires chemical processing with strong acids (HCl, H_2SO_4, HNO_3) or potentially with complexing agents (NH_3, chelants, organic acids), it becomes necessary to understand the solution chemistry and speciation of these metals at different pH's, concentrations, and anion types. This paper

[1] *https://price.metal.com/Rare-Earth*

explores the various extraction options from different ore sources for REE in which the chemistry of these elements has been studied.

New thermodynamic model

The Mixed Solvent Electrolyte (MSE) thermodynamic framework has been described in detail by Wang et al.[2,5], and therefore only a brief summary is given here. The two key components of an electrolyte (water-phase) model are the equation of state that predicts the thermodynamic properties of each species (G^0 H^0, S^0, V^0, Cp) as T and P vary, and the activity coefficient model that predicts the salinity (or non-ideal) effects on these same values (G^{EX} H^{EX}, S^{EX}, V^{EX}). This leads to computing the real Gibbs Energy of formation for each species using the basic equation:

$$G^{Real} = G^0 + G^{EX}$$

Equilibrium for a given reaction A=B can then be described as:

$$K = exp^{-\left([G_B^{Real} - G_A^{Real}]/_{RT}\right)} = \frac{B}{A}$$

For each species in water, the well-established, Helgeson-Kirkham-Flowers (HKF) equation of state is used to calculate G^0 and the new MSE framework is used to compute G^{EX}. A different set of equations are used to compute the vapor and hydrocarbon phase, but since they are not relevant to this paper, they are not discussed.

The MSE calculations include: (1) the formation of ion pairs, complexes, etc.(chemical speciation), (2) the effect of electrostatic charge on each species in water (activity coefficients), (3) the availability of free water to form hydrates, (4) the effect of solution chemistry on "secondary properties of water" such as viscosity, conductivity, density, osmotic pressures, etc. These calculation elements are used directly or indirectly to compute the solubility of REE phases and the speciation of REE ions in solution.

Limits on existing experimental data.

The sixteen rare earth elements (excluding Pm) coordinate/precipitate with any number of anions, notably: SO_4^{-2} (H_2SO_4 digestion), PO_4^{-3} (extraction from phosphogypsum), Cl^{-1} (HCl digestion and NaCl ion exchange), NO_3^{-1} (HNO_3 digestion), HCO_3^{-1}/CO_3^{-2} (Na_2CO_3 purification step), and OH^{-1} (water hydrolysis). The combination of sixteen REE and six anions result in ninety-six unique experimental sets of data.

Data availability is variable. For example, published data for Neodymium (Nd) is available for eight anions (including strong, weak, and organic acids). By comparison, data for Thulium (Tm) is limited to HCl. Thus, because experimental data is important for validating any simulation tool, the range of REE predictions vary: Nd, Eu, Tb can be predicted most extensively, whereas Er, Yb, and Lu can be validated in HCl and possibly H_2SO_4.

In addition to basic speciation data, challenges arise from data availability at different temperatures and salinities. For example, monazite, (Ce,La,Nd,Th)PO_4 is digested in H_2SO_4 or NaOH at up to 150 C[i]. Thus, Ce-SO_4, La-SO_4, Nd-SO_4, and Th-SO_4 interactions at these elevated temperatures are important to optimizing performance. REE extraction from phosphogypsum (PG) can also depending on methodology range in temperature. In both cases (or others) the thermodynamic constants for precipitation, complexation, and hydrolysis will differ from the standard 25 C temperatures. ~~Thus temperature effects on REE chemistry is also a necessary test.~~

We assume here, that four ore sources will satisfy current and future REE demand. Each source has their specific extraction routes or pathways[ii]: Monazite/Xenotime uses H_2SO_4 or NaOH digestion, Bastnasite uses HCl leaching or H_2SO_4 digestion[iii], and PG uses H_2SO_4 or HNO_3 digestion/leaching, or solvent extraction. Clays use NaCl or $(NH_4)_2SO_4$ for ion exchange[iv]. The additive chemistry is therefore limited to these anions, SO_4^{-2}, NO_3^{-1}, Cl^{-1}, and OH^{-1}, as mentioned above. The rock matrix also introduces anions PO_4^{-3}, SiO_3^{-2}, F^{-1}, and CO_3^{-2}. Lastly, extraction can extend to other ore sources, and thus complexing/precipitating agents like oxalic acid or extractive agents like tributylphosphate (TBP) become important. When the clay surface is considered, then a hypothetical surface group is needed to model the selectivity of REE for the surface compared to extracting metals (Na, K, Cs, Ba, Sr, Mg. Ca, etc.).

Table 1 – Extent of coverage for the REE. Green indicates that the system is studied, Yellow indicates that the system is estimated, and Red indicates that the system has not been studied (Das, 2017 and 2019).

REE	(OH)3	SO4	Cl	PO4	Org Acid	NO3	CO3	F
La								
Ce								
Pr								
Nd								
Sm								
Eu								
Gd								
Tb								
Dy								
Ho								
Er								
Tm								
Yb								
Lu								
Y								
Sc								

Using available data to make progress

This section is presented in detail by Gas et al.[v,vi] and a brief summary is provided here. To date, a portion of this chemistry has been measured and its thermodynamics quantified. Neodymium, perhaps due to its value, benefits from multiple experimental sources: forty with Cl^{-1}, eight with OH^{-1}, twelve with SO_4^{-2}, seven with CO_3^{-2}, and twenty-five with PO_4^{-3}. Thus, predicting $Nd(OH)_3$ (am. and cr.) solubility in water up to 250 C in and at multiple salinities is achievable. Das et al, did an an exhaustive study of available REE-sulfate properties and measurements. They list sixty-two references that provided or contributed to properties important to this chemistry.

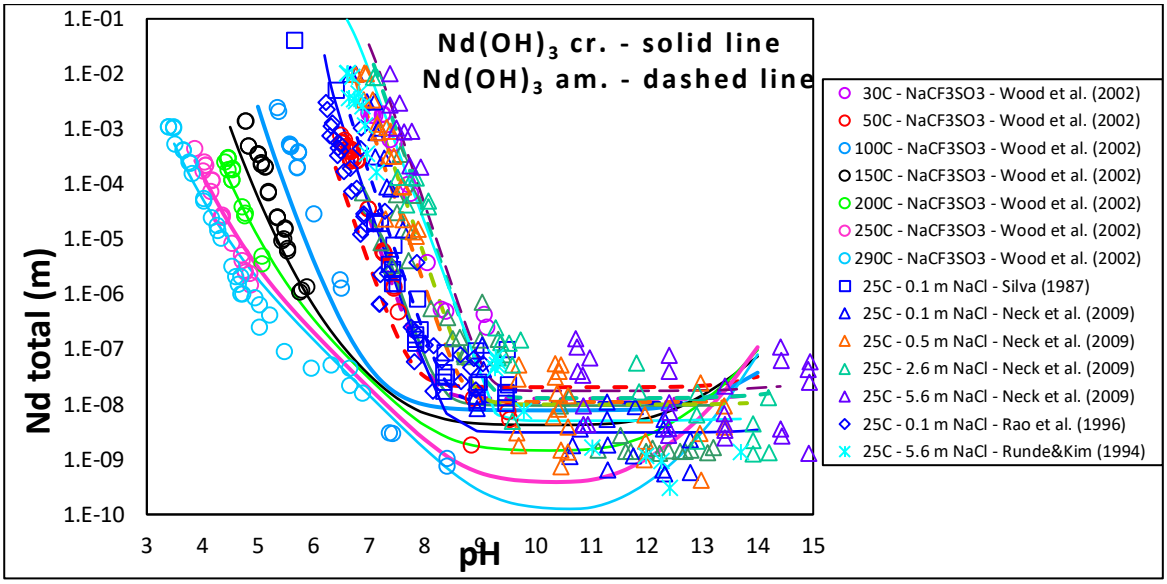

Figure 1 - Validation plot of $Nd(OH)_3$, (cr. and am.) vs pH, between 25 and 250C, and in different salt solutions. Symbols are experimental data and curves are model predictions. There is significant amount of data for Nd, which aids in developing more representative parameters.

Lutetium experimental data, by comparison is limited to Cl^{-1} (eleven references) and SO_4^{-2} (five references). Therefore, the extent to which a prediction can be validated is more limited. These conclusions are based on an extensive literature search for rare-earth elements chemistry performed over the past four years and published in part by Das et al. (2017 and 2019). The plot below displays $Lu_2(SO_4)_3$ solubility vs. temperature. two items are worth explaining, first is that the $Lu_2(SO_4)_3$ data we have found is for a fixed stoichiometric ratio 2:3, and the lutetium concentration in sulfate solutions is relatively high (>20,000 ppm below 100 C), and so its solubility in a solution of PG and acid

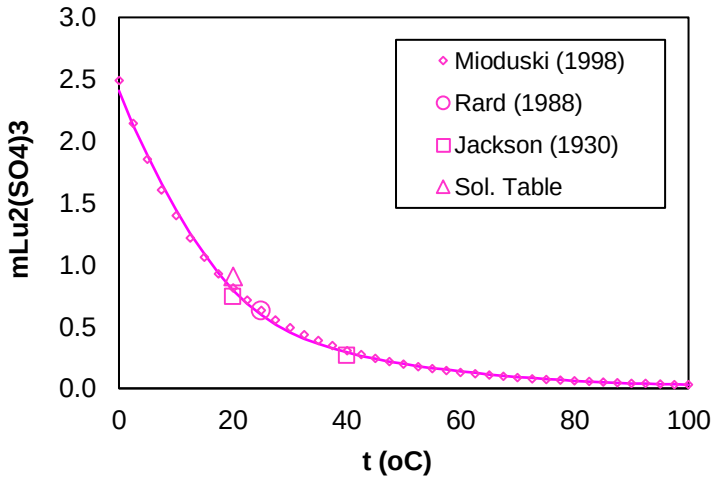

Figure 2 - Validation plot for $Lu_2(SO_4)_3$ vs temperature. Symbols are experimental data and the curve is model predictions. The limited data availability limits the prediction confirmation.

Thus, despite the limited amount of experimental data, solution/phase predictions of these elements in the extractive agents can be tested for some metals.

What we can see thus far

One result from the research is development of metal-hydroxide solubility curves for each REE. The plot below is the dissolved concentration of REE in pure water vs. pH and at 25C or 95 C. At both temperatures, the solubilities reach low levels (<1mg/l). However, the solubility at 95 C is

computed to be up to two orders-of-magnitude higher. Thermodynamic variabilities like this are useful when attempting to maximize extraction and separation.

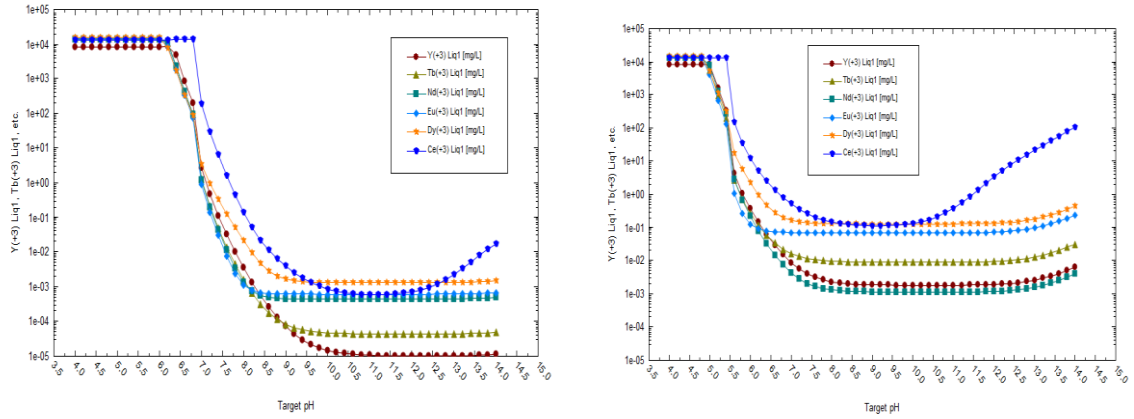

Figure 3 - computed solubility of six REE hydroxides vs. pH at 25 and 95 C. The solubility at 25 C is computed to be lower, and the precipitation is computed to occur at lower pH at 95C.

Another significant chemical transition is oxidation effects. Cerium is separated from other elements because it oxidizes to the Ce(IV) state and forms an insoluble CeO_2 precipitate. This precipitate is temperature and pH dependent, and therefore manipulating one or both can aid in extracting cerium more efficiently.

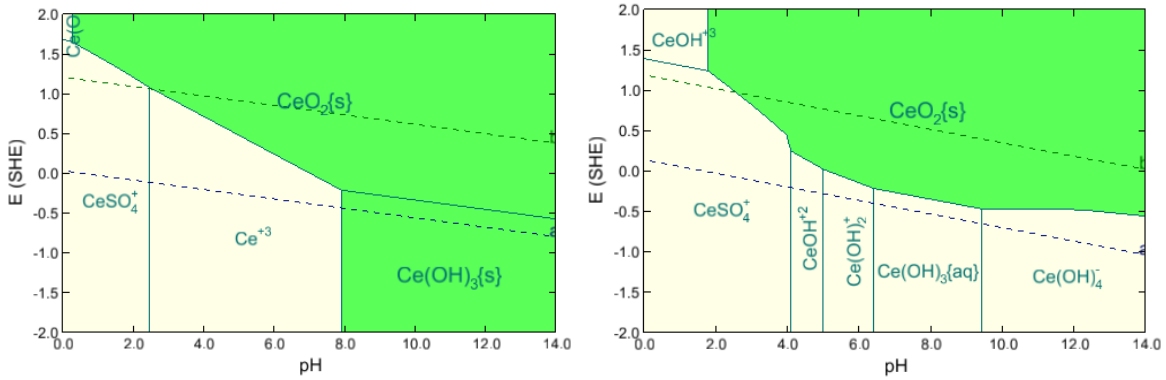

Figure 4 - Pourbaix diagram of Cerium in water at 25 and 150. H_2SO_4 is the digestion acid (below 7 pH). The Ce(III)-Ce(IV) boundary at ca. pH=0 decreases from +1.6V at 100C to +0.4V at 300, making it more susceptible to oxidation at higher temperatures.

A third chemical transition is the formation and loss of hydrates in REE salts. Figure 5 contains the experimental (and predicted) solubility of dysprosium chlorides as temperature varies from 1 to 160 C. Between -20 and 60 C, where most of the experimental data is available, solubility change is flat, increasing from ca. 3.5 to 4 mol/kg. Within this temperature region, three phases are computed to exist: fifteen-, nine-, and six-hydrate. Above 160, there are independent experimental datapoints that indicate a several-fold increase in $DyCl_3.6H_2O$ solubility. Conversely, at low temperature (e.g., <20 C), ice and $DyCl_3.15H_2O$ coexists, which may provide engineering options for low-temperature fractional crystallization.

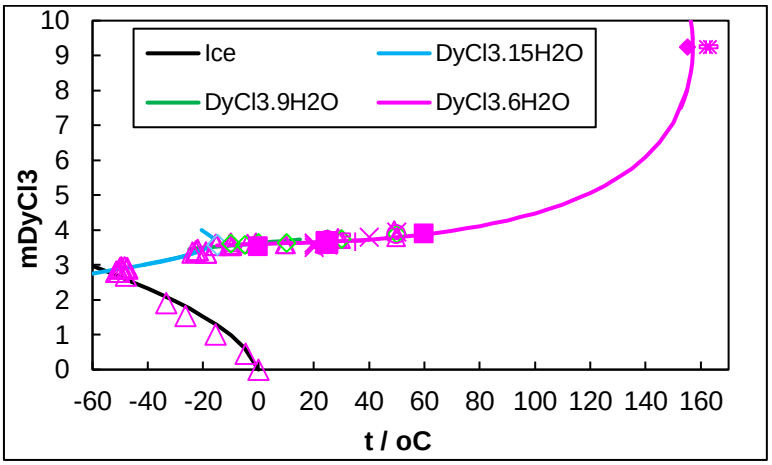

Figure 5 - Phase composition and solubility of dysprosium chlorides as a function of temperature. The symbols are expermental data (references available in Table 1 of Das et al. (2017). Lines are the (predicted) hydrated phases, including ice.

Extraction and purification predictions

The purpose of electrolyte-based, mass balance, process simulators is to model the extraction and purification process. The net effect is an optimization of the process. Based on the partial validation of REE with critical anions, the technology is not yet ready to do this in its entirety, but is able to focus on important systems, like the sulfates, chlorides, and hydroxides.

The software tool used is from OLI Systems, Inc. (Cedar Knolls, NJ), version 9.6.2. The tools used included a flash calculator and a steady-state process simulator. No rate-limiting reactions were included, and therefore all results are at equilibrium state. Equilibrium state will limit the interpretation when the leaching experimental results display rate limiting properties.

The REE solid phases considered are too numerous to list but can be inferred using Table 1. Phases that form will be described in the results section.

We will present the following extraction processes where much of the chemistry is validated. The processes include PG digestion with H_2SO_4 and bastnasite roasting and acid leaching. The simulations are equilibrium based, meaning that the kinetics of digestion, leaching, and element mobilization is not considered. We will also discuss where we think additional data or mechanisms are needed.

Phosphogypsum digestion

Starting material

The first simulation is of REE extraction from PG cake, the byproduct of the dyhydrate process in phosphoric acid production. The hypothetical cake composition is based on a US Department of energy report[vii] contains (on a mass % or ppm basis). The SO_4^{-2} and H_2O content was not provided, but information about total gypsum content (72%) was reported. Total sulfate was back

calculated from electroneutrality and the proton balance was back calculated using a free-water pH of 5.5. Lastly, to simplify the plots, light REE (LREE) were simulated using Nd and heavy REE (HREE) were simulated using Y.

Table 2 - Phosphogypsum composition used in this study[viii]. The computed equilibrium phases for these components.

Oxide	Mass%	Element	Ppm	Phase	Mass%	Phase	ppm
P_2O_5	0.99	Y (HREE)	70	$Ca(REE)SO_4.2H_2O$	92.7	YPO_4	110
CaO	22.65	Nd (LREE)	150	$Ca_5(PO_4)_3F$	3.5	$NdPO_4$	180
Fe_2O_3	0.13			CaF_2	2.8	UO_2	55
Al_2O_3	0.22			$Al(OH)_3$	0.5		
HF[2]	1.06			FeO(OH)	0.2		
H_2SO_4	35[3]						
H_2O	40[4]						

Three REE configurations are reported in PG : 1) substitution for calcium or calcium -sulfate in the gypsum lattice; 2) adsorption on the PG matrix surface; and 3) as a separate phosphate phase.

We assume that 30% of the REE is in the first configuration; substituted for Ca^{+2} in gypsum and has the formula $Ca_{0.99963}(REE_{0.00037})SO_4.2H_2O$ (herein $Ca(Nd,Y)SO_4.2H_2O$ or RE-Gypsum) and 70% is $NdPO_4$ and YPO_4. With respect to the $Ca(Nd,Y)SO_4.2H_2O$ phase, we assume congruent dissolution and no difference in thermodynamic properties (G, H, S, V, Cp) compared to pure gypsum.

Simulation approach

The simulation is based on the 120-minute leaching experiment described in the OSTI report. Three-hundred grams of dry PG (Table 2) and 1200 g H_2O is mixed at 50 C to create the slurry. Between 0 and 30 grams of 100% H_2SO_4 is then added to the slurry at 3 g increments. All potential solids can reprecipitate except for $CaSO_4$, $CaSO_4.0.5H_2O$ and $CaSO_4.2H_2O$. The assumption is that pure calcium sulfate phases will not reprecipitate in the presence of a REE-containing liquid.

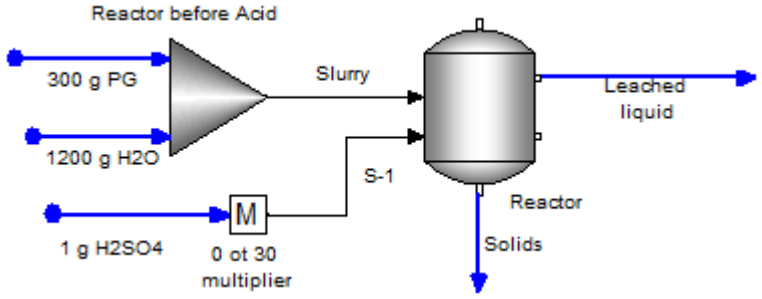

Figure 6 - Configuration of the Leaching simulation. 300 g PG is mixed with 2500 g H2O. This is then reacted with between 0 and 30 g pure H_2SO_4

The mass of dissolved P, F, Nd, Y, and U in the leached liquid stream and the mass of each solid phase in the solid stream is documented at each simulation step.

Simulation results using H_2SO_4

Figure 7 is the comparison of the OSTI results (their Figure 1) and this simulation results. According to the OSTI report, about 40% of the REE is leached during digestion. Fluoride and P_2O_5 leaching is 70% and 80% respectively.

---

[2] H^+ assumed to be the counterion for F^{-1} and SO_4^{-2}, based on the use of oxides for metal (alternative is Na^+)
[3] Anion balance.
[4] 2 moles H2O per mole Ca (gypsum) plus moisture balance to 100 % mass.

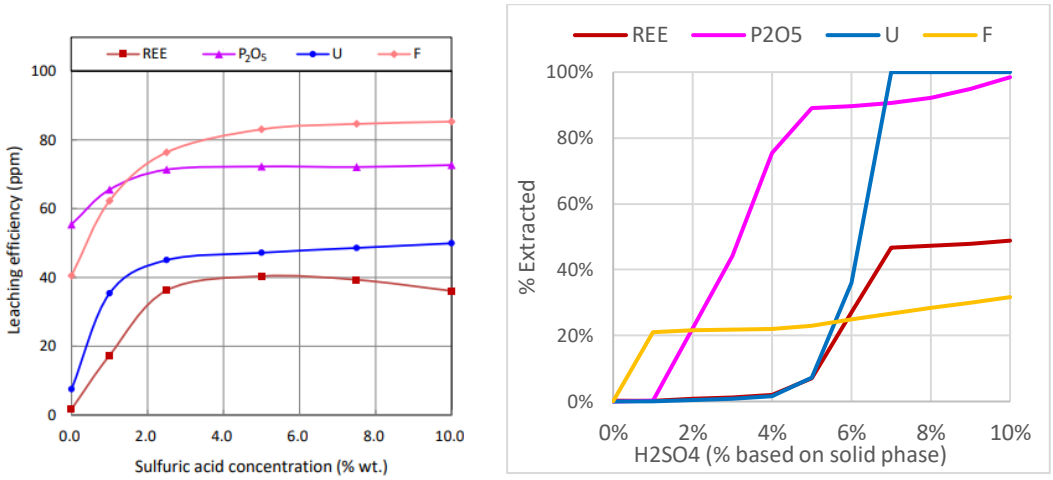

Figure 7 – (Left) Plot from OSTI report showing the leaching efficiency (percent not ppm) of four key components in PG as H_2SO_4 is added up to 10%. The digestion is at 50 C and for 160 minutes. (Right) Plot of the simulated digestion at 50 C.

When our results are compared, the expected acid-dissolution reaction trend is present, but there are differences in the values. For example, F dissolved to about 30% (compared to 80%) and U dissolves to 100% compared to their 50%. There is limited agreement with dissolved P (85% vs 65%) between 4 and 7% H_2SO_4 addition, but it is simulated to dissolve completely by 10%.

The simulated leach solution also displays a lag in the leached concentrations. The OSTI results display concentration plateaus at 2-4% H_2SO_4. Our simulation displays plateaus at about 5-6%. The main cause of this difference is because $NdPO_4$ and YPO_4 are computed to dissolve completely by 7% and the released calcium is computed to reprecipitate as $Ca(Nd,Y)SO_4.2H_2O$.

Figure 8 contains the mass of each phase remaining at each leaching step. The weak acid salts ($Ca_5F(PO_4)_3$, $Al(OH)_3$, $FeO(OH)$, CaF_2, $NdPO_4$, and YPO_4) dissolve, releasing REE, Ca, P, and F into solution. This is computed to be complete by 7% H_2SO_4. The dissolved calcium, REE, and sulfate reprecipitate as RE-Gypsum. This phase mass is computed to increase from the initial 275 g to 297 g by ~5% H_2SO_4 solution. Beyond this point, all available Ca^{+2} is consumed, and no additional $Ca(Nd,Y)SO_4.2H_2O$ forms.

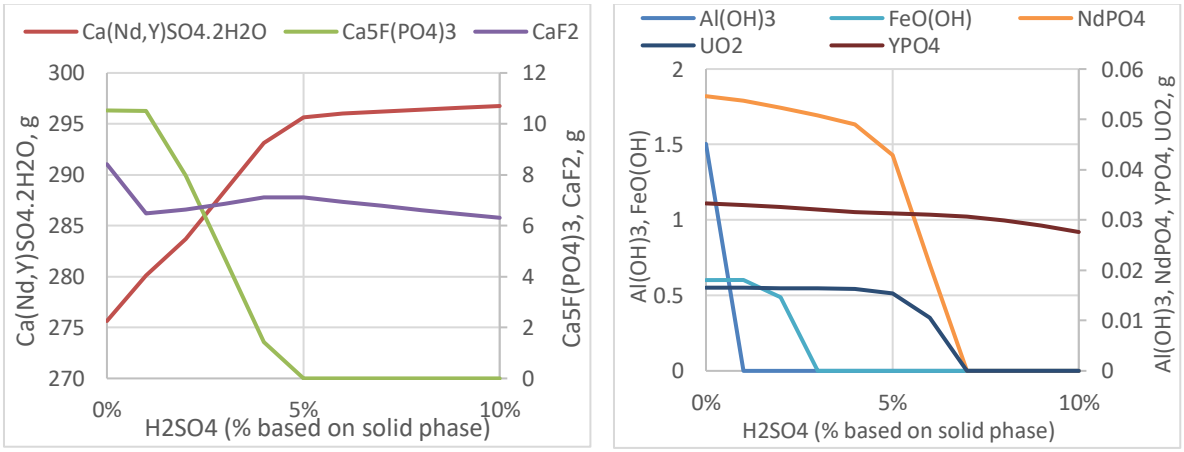

Figure 8 - Plot of the solids present in the simulated leaching reactor as H_2SO_4 is added to the slurry. The data are displayed in two figures because of the different scales in

If $Ca(Nd,Y)SO_4.2H_2O$ reprecipitation does not occur, then the REE plateau occurs at lower 5% H_2SO_4 instead of 7 (Figure 9). This is still higher than the OSTI results and may be due to the assumed phase composition used in Table 2.

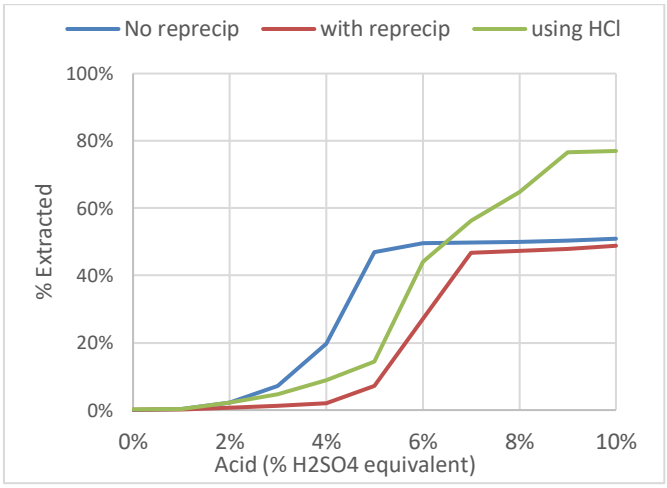

Figure 9 - Percent of REE extracted from PG when $Ca(Nd,Y)SO_4.2H_2O$ does or does not precipitate from the leach solution. Also, the effects of using HCl instead of H_2SO_4 is shown.

Any reprecipitation can also be obtained by measuring the dissolved calcium and sulfate concentrations (Figure 10). If reprecipitation is occurring (as any form of gypsum), then the dissolved calcium and sulfate concentration should increase non-linearly. The OSTI report did not contain dissolved calcium and sulfate data, and therefore the reprecipitation reaction cannot be confirmed.

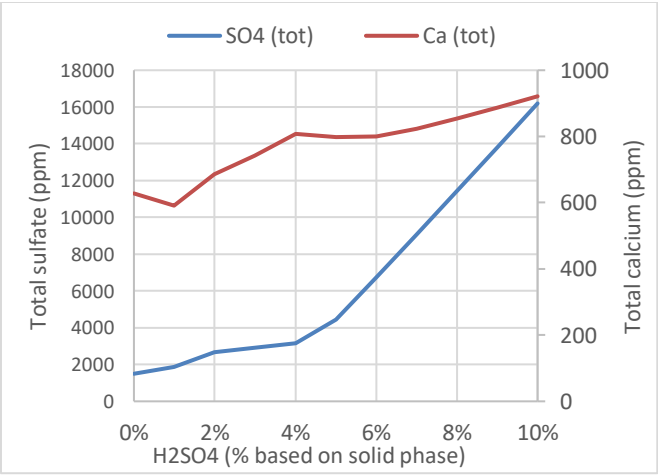

Figure 10 - Plot of the computed dissolved sulfate and calcium in the slurry, and the computed effect of calcium sulfate precipitation cause by H_2SO_4 addition

Simulation results using HCl

Figure 9 also contains the effects of using HCl instead of H_2SO_4 as the leach solution. Based on these simulations, REE extraction exceeds 70% because the gypsum matrix is attacked by HCl, releasing REE. This is shown in Figure 11, where remaining $Ca(Nd,Y)SO_4.2H_2O$ mass is plotted against the acid is added. Increasing mass results in REE sequestration.

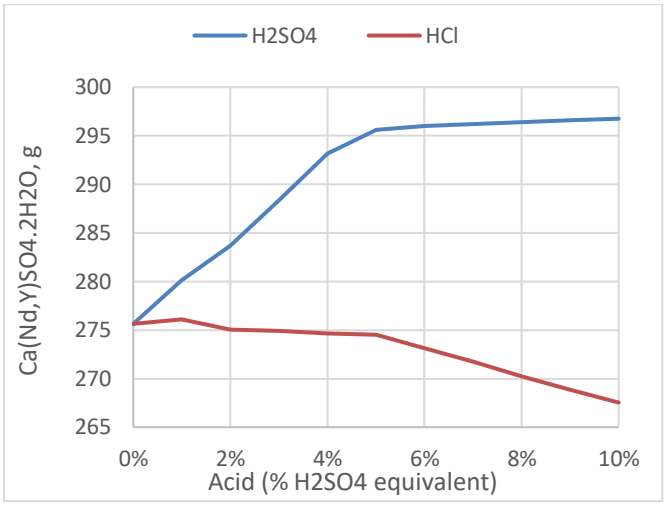

Figure 11 - The computed mass of $Ca(Nd,Y)SO_4.2H_2O$ present in the slurry when the acid is changed from H_2SO_4 to HCl

Summary of phosphogypsum simulation.

The initial conclusion from this work is that equilibrium speciation and phase formation can provide some indication of REE extraction from PG. These predictions need an assumed value of REE distribution in the gypsum (30% in this simulation), as a phosphate phase (70%), or adsorbed onto existing solids (0%). Also required, is the elemental analysis of the PG ore. Lastly, measuring the leached solution for marker ions like calcium can help determine the extent of dissolution and reprecipitation process.

Processing Bastnasite ore

Gupta and Krishnamurthy[ix] provide a review of Bastnasite processing reported in Kruesi and Duker (1965). In this process, ore concentrate is attacked with HCl to produce REE fluorides salts and an REE-rich liquor is decantated. The REE fluorides are converted to REE-hydroxides using NaOH, and the NaF-rich liquid is removed from the process. The REE-hydroxides are sent back into the process to neutralize the HCl-rich liquor. The slightly acidic solution is treated to remove Th, Ba, Pb, and Fe in a waste filter cake and the remaining liquor is concentrated to produce REE-chlorides.

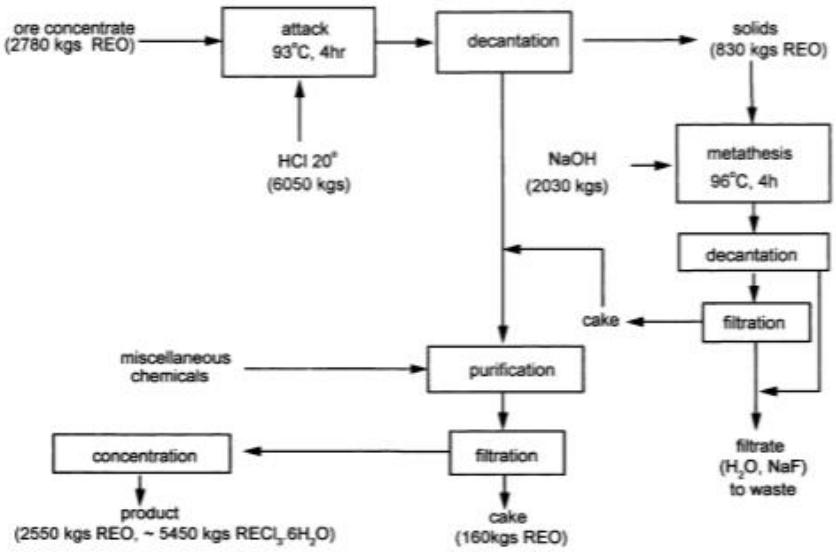

Figure 12 – REE purification process from bastnaesite ore concentrate as reported in Figure 3.16 of Gupta and Krishnamurthy (2005). They reported the work of Kruesi and Duker (1965). The main reagents are HCl and NaOH.

This process was modeled using the data provided in the reference

*Table 3 - Bastnasite ore concentrate used in the simulation (adapted from Table 3.1 of Gupta and Krishnamurthy, 2005). *The F content was increased from 5.5 to 11% so that sufficient fluoride existed to precipitate the reported mass of REO solids*

Component	Percent	Component	Percent	Component	Percent
$BaSO_4$	0.75	ThO_2	0.01	Sm_2O_3	0.62
CaO	0.75	CeO_2	50	Eu_2O_3	0.11
F (as HF)	11*	La_2O_3	31	Gd_2O_3	0.2
Fe_2O_3	0.4	Pr_6O_{11}	5	Y_2O_3	0.05
SiO_2	0.75	Nd_2O_3	12.9		

Simulation approach

A steady state process simulator package (OLI Flowsheet V962, OLI Systems, Inc.) was used to model this process. In addition to the basic thermodynamic database, a pseudo-database labeled REEXT developed by AQSim, Inc. (Denville, NJ) containing speciation and solid phases estimations for REE-fluorides was also used. This database contains reference thermodynamic properties (G, H, V, Cp) from various peer-reviewed sources[xxi], but have not been validated using experimental data. Using this database was necessary for simulating the first step of this purification process. This database will eventually be replaced with a validated database.

Figure 13 is the schematic of the process simulated. 3218 kg of ore concentrate containing 2780 kg REO is mixed with 5380 kg of 20 Baume HCl at 93 C. Since the calculations are equilibrium, no reaction time is used. The acidified mixture contains 850 kg rare earth fluorides (REF_3) of CeF_3, PrF_3, and SmF_3 solids, which is separated from the liquor in the Decantation step. A KOH (30%) and NaOH (3%) caustic solution is added to the solids to convert the REE to hydroxide form. The solubilized fluoride is removed in the filtration step. The hydroxide solids are mixed back with the decantant to raise the pH to about 4. At this pH, ThO_2, $Fe(OH)_3$, and CaF_2 impurities precipitate and are removed. A significant amount of $La(OH)_3$ is also computed to be removed in this step. Lastly, the filtrate is evaporated to near dryness at ambient temperatures with air to form rare earth chloride (RECL3) salts.

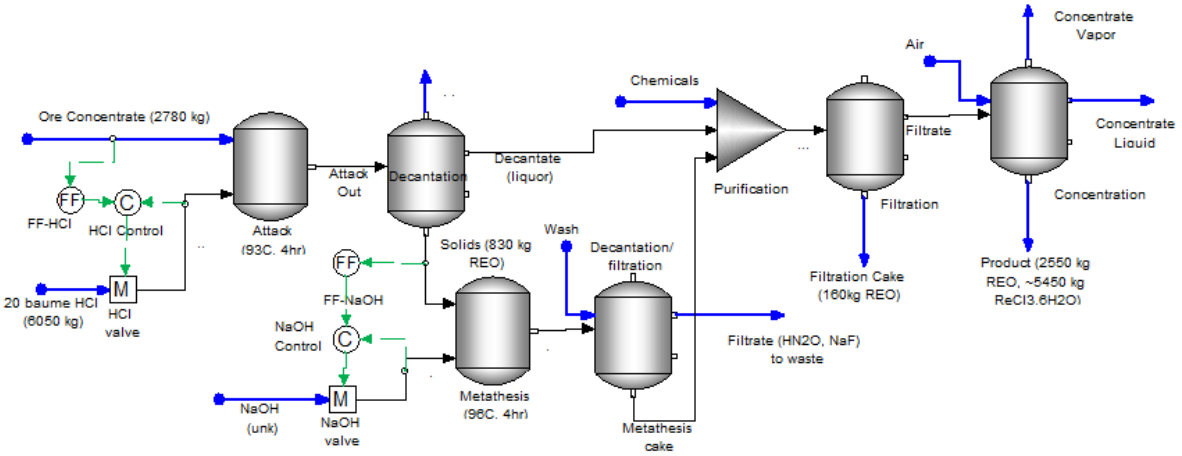

Figure 13 - Schematic of the simulation.

Table 4, below contains a comparison of the available reported data and the simulated results. Most values are in good agreement. Less acid and caustic are computed to be required to achieve the same target outputs. Also, the required fluoride content in the ore is key to matching design results, but this is not a requirement, since 90+% of the fluoride in the ore is computed to precipitate with REE. A different mass of REF_3 would change the caustic demand, which would need to be made up later in the process.

Table 4 - Comparison between reported production rates and computed values.

Step	Reported	Computed	Step	Reported	Computed
Ore concentrate as REO (kg)	2780	2780	Cake wash water (kg)		5000
Total ore (kg)		3180	REO in meththeis cake		996
F in ore (wt%)	5.5	10	Purification pH	3	4
20 Baume Acid used (kg)	6050	5382	REO in Filter Cake	160	100
Fluoride solids (kg as REO)	830	1000	REO in Product	5450	5726
Caustic makeup	NaOH	KOH,NaOH			
Caustic added (kg/kg ore)	500	292			

In our simulation, we observed that a using NaOH in the metathesis step causes NaF salts to form. These salts would be sent with the REO cake back to the process. Therefore, a 90:10 KOH:NaOH mixture was used instead. This would in turn change the caustic demand, which Notable about the reasonably good fit, is the ability of Kruesi and Duker to produce a similar mass balance over fifty-years before a thermodynamic database and simulator was available to confirm their values.

Summary of bastnaesite simulation

There is reasonable comparison between the reported and simulated values for this process. The overall mass balance of the REO is confirmed and the amount of REF_3 formed in the decantation step will be a function of the fluoride content in the ore. The HCl and NaOH requirements can be optimized and the selection of NaOH or KOH is based on maintaining the purity of the metathesis cake. Lastly, the effect of temperature on the overall REO, REF3, and RECL3 solubility can be incorporated into the optimization step.

The development of thermodynamic properties for REE chlorides and oxides has enabled partial simulation of the digestion and purification of bastnaesite concentrate ore using HCl, KOH, and NaOH. rare earth ores. We simulated the digestion, purification, and concentration step using a REE database that is validated from experimental data. We simulated the decantation and metathesis steps using a database created from reported thermodynamic properties but not validated with experimental data.

Conclusion

A thermodynamic database is being developed to predict the aqueous and solid-phase properties of sixteen rare earth metals. The database is partly complete, and contains validated parameters for hydroxides, sulfates, chlorides, and for some elements, phosphates, nitrates, carbonates, and organic acids.

The simulation output was tested against two reported processes, phosphogypsum extraction and bastnaesite purification. Each process requires a different rare-earth chemistry and offers a test to the model accuracy. Reasonable agreement was found in both simulations, considering the limits of equilibrium modeling to predict rate-limited processes.

Abbreviations

REO	Rare earth oxides	PG	phosphogypsum
REE	Rare earth elements	RE-Gypsum	$Ca_{0.99963}(REE_{0.00037})SO_4.2H_2O$ and $Ca(Nd,Y)SO_4.2H_2O$
RECL3	Rare earth chlorides	LREE	Light rare earth elements
REF3	Rare earth fluorides	HREE	Heavy rare earth elements
		OSTI	US DOE report on REE recovery (see ref)

References

[i] M.K. Jha, A.Khumari, R. Panda, J.R. Kumar, K. Yoo, and J.Y. Lee. 2016. Review on hydrometallurgical recovery of rare earth metals. Hydrometallurgy. 165, p2-26.
[ii] Ibid.
[iii] M.K. Jha, A.Khumari, R. Panda, J.R. Kumar, K. Yoo, and J.Y. Lee. 2016. Review on hydrometallurgical recovery of rare earth metals. Hydrometallurgy. 165, p2-26.
[iv] V. Papangelakis, and G. Moldoveanu. 2014. Recovery of rare earth elements from clay minerals. ERES2014: 1st European Rare Earth Resources Conference|Milos|04-07/09/2014.
[v] Das, Gaurav., M.M. Lencka, A. Eslamimanesh, P. Wang, and A. Anderko. 2019. J. Chemical thermodynamics. 131, p49-79.
[vi] Das, Gaurav, M.M. Lencka, A. Eslamimanesh, A. Anderko, and R. Riman. 2017. Rare earth elements in aqueous chloride systems: thermodynamic modeling of binary and multicomponent systems in wide concentration ranges. Fluid Phase Equilibria. 452, p16-57.
[vii] Liang, Haijun, Zhang, Patrick, Jin, Zhen, and DePaoli, David W. 2017. Rare earths recovery and gypsum upgrade from Florida phosphogypsum. United States:. Web. doi:10.19150/mmp.7860. https://www.osti.gov/pages/servlets/purl/1437893
[viii] Ibid.
[ix] Gupta, C.K., N. Krishnamurthy. 2005. Extractive metallurgy of rare earth. CRC Press. 484 pp.
[x] Haas, J.R., Shock, E.L, Sassani, D.C. 1995. Rare earth elements in hydrothermal systems: Estimates of standard partial molal thermodynamic properties of aqueous complexes of the rare earth elements at high pressures and temperatures. Geochim. Et Cosmochim. Acta 59(21) 4329.
[xi] Glushko, V.P, Medvedev. V.A., Alekseev, V.I.m, Bergman G.A., Vasil'ev, B.P. Khodakovskii, I.L., Gurvich, K.V>, Yungman, V.S., Reznitskii, L.A., Kolesov, V.P., Vorob'ev, A.F., Tatsimirskii, K.B., Smirnova, N.L, Biryukov, B.O, Gal'chenko, G.L, Ioffe, N.T., Baibuz, V.F.. 1978. Thermal Constants of compounds. Academy of Sciences, USSR.